Polskie Towarzystwo Materiałów Kompozytowych
Polish Society of Composite Materials

26: 2 (2026) 152–159

COMPOSITES THEORY AND PRACTICE

ISSN (online): 2299-128X

Tadeusz Kubaszek, Barbara Kościelniak, Marek Góral*, Agnieszka Zielinska, Kamila Świerk

Research and Development Laboratory for Aerospace Materials, Rzeszow University of Technology, Powstancow Warszawy 12, 35-029 Rzeszow, Poland
* *Correspondence*: mgoral@prz.edu.pl

Received (Otrzymano) 20.05.2026
Published on-line (Opublikowano) 30.06.2026

THE INFLUENCE OF PLASMA SPRAYING PROCESS PARAMETERS ON MICROSTRUCTURE AND SELECTED PROPERTIES OF NOVEL NiCr-YSZ COMPOSITE COATING

https://doi.org/10.62753/ctp.2026.09.2.2

This study investigates the influence of the atmospheric plasma spraying (APS) parameters on the microstructure, mechanical properties, and tribological performance of novel NiCr–YSZ (70/30 wt%) composite coatings. Coatings were deposited onto S235 steel substrates with varying current intensities (300, 500, 700 A) and hydrogen flow rates (4, 8, 12 NLPM). Microstructural analysis revealed that increasing the current to 700 A and hydrogen flow to 8–12 NLPM enhanced particle melting, producing dense coatings with minimal porosity (0.77 vol.%), while reduced hydrogen flow (4 NLPM) resulted in incomplete YSZ particle melting, increased porosity (3.17 vol.%), and a decreased coating thickness (~307 µm). The mechanical and tribological properties correlated strongly with the coating density. The highest hardness (413 HV0.2) and lowest erosion mass loss (0.00703 g) were achieved at 700 A and 12 NLPM. The specific wear rate ranged from 8.25×10^{-5} to 1.36×10^{-4} mm³/(N·m), with the lowest value corresponding to the densest microstructure produced at an elevated current intensity. The coatings deposited at 300 A or 4 NLPM exhibited inferior performance due to increased porosity and weak interlamellar cohesion. These findings demonstrate that optimization of the APS parameters to 700 A and 8–12 NLPM enables the production of ultra-dense NiCr–YSZ coatings with superior resistance to erosion and sliding wear, suitable for demanding erosive–abrasive applications.

Keywords: plasma spraying, NiCr-YSZ coatings, erosion, wear resistance, hardness

INTRODUCTION

The advancement of modern technologies in the aerospace, energy, and mechanical engineering sectors necessitates the development of coatings simultaneously resistant to intense wear, cavitation, and corrosion [1–4]. A key solution in surface engineering represents coatings based on an NiCr matrix, which – owing to their high thermal and chemical stability – constitute a foundation for composite materials reinforced with hard carbide and oxide phases. Ni–Cr coatings themselves, particularly at a weight ratio of 80/20, provide high oxidation resistance through the formation of “glaze”-type oxide layers. Tribological studies have demonstrated that above a transition temperature (150–200°C), oxidation products undergo densification, which significantly reduces the coefficient of friction by eliminating direct metal–metal contact. Contemporary NiCr coatings deposited by atmospheric plasma spraying (APS) are characterized by a density of approximately 5.46 g/cm³, porosity below 1.5%, and hardness of around 810 HV [6]. In thermal barrier coating (TBC) systems, the Ni–20Cr alloy is employed as a bond coat on nickel-based alloys and intermetallic substrates (e.g. TiAl), providing high adhesion (12.89 MPa) and effective accommodation of thermal stresses arising from mismatches in the coefficient of thermal expansion [7, 8]. Where high wear resistance is required, the matrix is typically reinforced with hard carbide particles. Typical NiCr–WC coatings produced by high velocity oxygen fuel (HVOF) spraying achieve hardness values of approximately 1403 HV0.3 and an indentation toughness of 2.7 ± 0.64, representing a 72% increase compared to alternative nickel-based systems [9]. In a 3.5% NaCl environment, these coatings exhibit excellent corrosion stability. NiCr–Cr_3C_2 coatings, in turn, demonstrate optimal tribological performance at 700°C owing to the dispersion of secondary carbides [2]. The application of two-phase structures in carbide coatings enables structural sealing (porosity ~0.75%) and reduces hot corrosion rates by nearly 60% [10]. An important direction of development involves oxide-reinforced composites exhibiting exceptional high-temperature strength. NiCr–Al_2O_3 systems display increasing hardness with a ceramic phase content (reaching ~1600 HV at 60 wt.%) and outstanding mechanical stability – the NiCr–40% composite retains a compressive strength of 540 MPa even at 1000°C [11]. The detonation spraying of multilayer gradient NiCr coatings enables hardness values of up to 15.9 GPa to be obtained [12]. Alternative NiCr–YSZ (yttria-stabilized zirconia) systems dominate TBC technology. The tetragonal YSZ phase exhibits high stability during isothermal oxidation up to 1050°C [7]. The application of additive manufacturing techniques, such as laser engineered net shaping (LENS), for such coatings allows the production of functionally graded materials, eliminating macroscopic interfaces and withstanding up to 240 thermal cycles at 1100°C [13, 14], while enabling a substrate temperature reduction of approximately 350°C.

The presented literature review [11–14] indicates that NiCr coatings with ZrO_2, Al_2O_3, and YSZ oxide additives are primarily used as heat-resistant coatings. They are rarely employed as substitutes for wear- and erosion-resistant coatings in which tungsten and chromium carbides are used as the reinforcing phase. In our research, we investigated the possibility of utilizing yttrium-stabilized zirconia as the strengthening phase. Due to the lack of literature and technical data, it is necessary to develop the spraying parameters for the new powder composition and to determine the effect of selected spraying parameters on the basic properties of NiCr–YSZ coatings.

EXPERIMENTAL PART

The NiCr–YSZ coatings were deposited onto a carbon steel substrate (S235). Prior to spraying, the sample surfaces were subjected to abrasive blasting (grit blasting) in order to develop surface topography and enhance mechanical adhesion, followed by cleaning in an ultrasonic bath. The coating feedstock consisted of a mixture of two commercial powders: 70 wt% NiCr matrix (Metco 43VF-NS) and 30 wt% ceramic reinforcement in the form of zirconia stabilised with 7.5% yttria (Metco 6700 YSZ). The coatings were produced by means of a plasma spraying system manufactured by Thermico (Germany), equipped with a single-electrode A60-type torch. The following parameters were adopted as the reference (standard) conditions: current intensity 500 A, hydrogen flow rate 8 NLPM (normal liters per minute), argon flow rate 66 NLPM, powder feed rate 20 g/min, carrier gas flow rate 6 NLPM, and spray distance 100 mm. The variable parameters were the current intensity (300/500/700 A) and hydrogen flow rate (4/8/12 NLPM). These parameters were selected based on prior experimental studies [15]. Microstructural characterization was performed on cross-sectional specimens using optical microscopy (Leica 3000) and scanning electron microscopy (Phenom XL). The porosity was evaluated by computer-assisted image analysis (Met-Ilo software) over ten representative areas. The chemical composition analysis and elemental mapping (EDS) were conducted at an accelerating voltage of 15 kV.

Hardness measurements were carried out on prepared metallographic cross-sections employing a Nexus 4303 hardness tester (Innovatest). The Vickers method was applied with a load of HV0.2 (1.96 N) and a dwell time of 10 s. For each sample, a series of five measurements was performed, and the average coating hardness values were calculated.

Erosion resistance was evaluated in accordance with ASTM G76 utilizing a TR-470 apparatus (Koehler) at a temperature of 25°C. The samples were machined to fit the specimen holder of the device. Each test lasted 10 minutes per specimen. The mass of each specimen was measured before and after testing. The powder feed rate was set at 2 g/min with an oŋ pressure of 0.2 kg/cm². The erosion resistance was assessed for specimens positioned at an angle of 90° relative to the nozzle. Mass measurements were performed by means of an analytical balance (KERN ABT 120-4M) with an accuracy of 1×10^{-4} g.

Tribological properties were evaluated using the ball-on-disc method with a T-01M tribotester, following the ASTM G99-17 standard. The adopted parameters included a linear speed of 0.1 m/s, a load of 30 N, and a sliding distance of 500 m. A tungsten carbide (WC) ball with a diameter of 10 mm and a hardness of 1741±5 HV10 was used as the counterbody. Based on the geometry of the wear track, the material volume loss was determined according to standard recommendations. The wear track width was measured utilizing an MM20 (Cs-Creative Solution) optical microscope and Capture 3.0 image analysis software. The specific wear rate, k, was calculated according to Equation 1:

$$k = \frac{V}{Fn \cdot L} \tag{1}$$

where:

k – specific wear rate [mm³/Nm)]

V – wear volume loss [mm³]

Fn – applied normal load [N]

L – total sliding distance [m]

RESULTS

Microstructure, porosity and chemical composition of coating

Metallographic analysis of the NiCr–YSZ composite coatings deposited by APS revealed a heterogeneous, lamellar microstructure typical of thermal spray processes, characterized by the presence of flattened particles (so-called splats), interlamellar boundaries, and oxide inclusions (Fig. 1a).

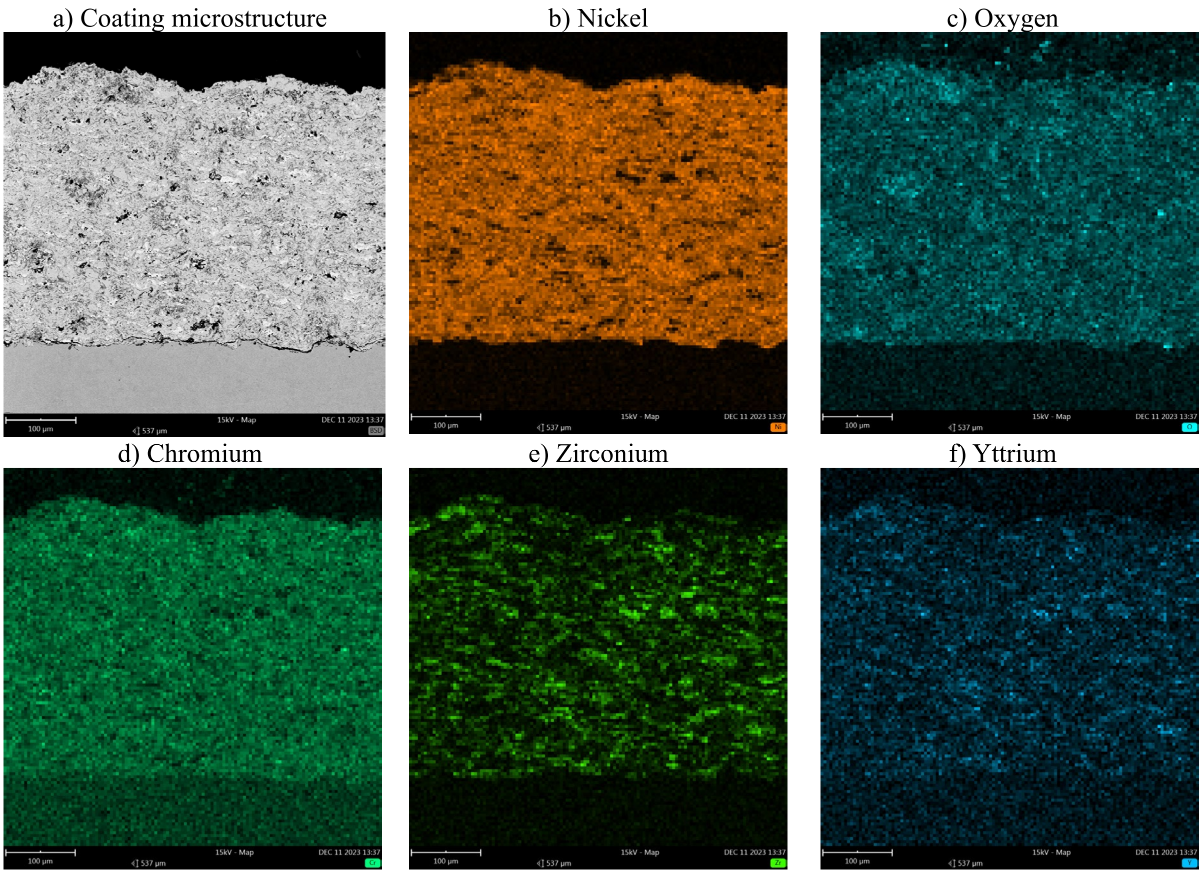

Fig. 1. Microstructure of plasma-sprayed NiCr-YSZ coating (standard parameters 8 NLPM H2, 500A) (a) and elemental mapping of b) nickel, c) oxygen d) chromium, e) zirconium f) yttrium

In the samples sprayed under standard parameters (500 A, 8 NLPM) and an elevated power current (700 A), a high degree of particle melting was observed, resulting in the formation of dense lamellae with a low content of structural defects. This effect is attributed to the increased kinetic and thermal energy of the particles, promoting their intensive melting and plastic deformation upon impact with the S235 steel substrate. Consequently, porosity was minimized, reaching the lowest value of 0.77 vol.% at the higher current intensity (Fig. 2a). As reported by Jiao et al. [10], porosity reduction in NiCr-based coatings is critical for limiting the diffusion pathways for corrosive media and improving interfacial cohesion. An opposite trend was observed with a reduced hydrogen flow rate (4 NLPM). Hydrogen, owing to its high thermal conductivity, significantly increases plasma enthalpy. Its deficiency leads to insufficient melting of the ceramic YSZ particles, which is reflected in the microstructure by the presence of numerous undeformed, spheroidal grains, increased porosity, and a reduced coating thickness of approximately 307 μm, with porosity rising to 3.17% (Fig. 2b). According to Savitha et al. [14], the presence of unmelted ceramic particles within a metallic matrix may result in local discontinuities and mechanical weakening of the coating due to particle pull-out during service. The coating thickness ranged between 370 and 380 μm, except for the coating produced at the lowest hydrogen flow rate (Fig. 2a, b).

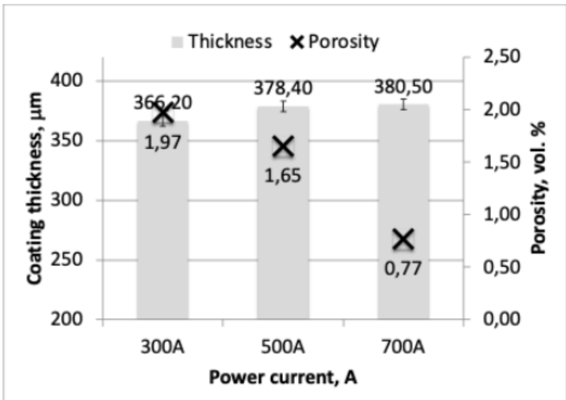

a)

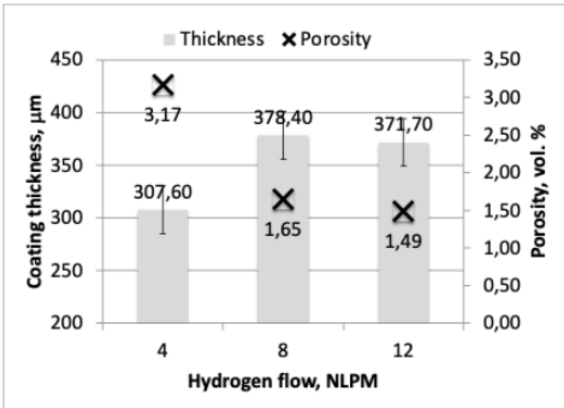

b)

Fig. 2. The influence of power current (a) and hydrogen flow (b) on thickness and porosity of plasma-sprayed NiCr-YSZ coating

The elemental mapping by means of energy-dispersive X-ray spectroscopy (EDS) analysis performed on the coating produced under standard spraying parameters confirmed the presence of the principal constituents of the system, namely Ni, Cr, Zr, O, and Y (Fig. 1). The elemental mapping revealed distinct phase segregation, arising from the composite nature of the feedstock material (70% NiCr / 30% YSZ). The distribution of nickel revealed regions of depletion, correlating with the location of ceramic particles enriched in zirconium and yttrium. Zirconium and yttrium were observed in the form of stable agglomerates, indicating the spheroidal morphology of the Metco 6700 powder, which retains partial structural stability within the plasma jet despite the high processing temperature. The oxygen map indicated its presence associated both with YSZ oxides and oxide regions within the NiCr matrix, attributed to in-flight oxidation – primarily chromium oxidation during particle flight – leading to the formation of passivating oxide layers. Doleker et al. [7] suggest that the local presence of chromium oxides may exert a reinforcing effect in thermal barrier coatings (TBCs); however, their excessive accumulation may increase the brittleness of metallic lamellae.

Hardness

The hardness of the coatings demonstrated a strong dependence on the process parameters. An increase in both the torch current and the hydrogen flow rate resulted in a corresponding rise in coating hardness (Fig. 3a and b). The highest hardness was obtained for the coating produced at the elevated current of 700 A, reaching 413 HV0.2 (Fig. 3a). The lowest hardness value (353 HV0.2) was recorded for the H variant, which is associated with increased porosity and weak interlamellar cohesion (Fig. 3b). The obtained values are significantly higher than those reported for bronze-based composites reinforced with YSZ (160–170 HV0.2), which can be attributed to the inherently higher hardness of the NiCr matrix [16]. Nevertheless, these values remain lower than those of dense, monolithic NiCr coatings [6], which may be explained by the dispersion of the ceramic phase and the presence of microporosity.

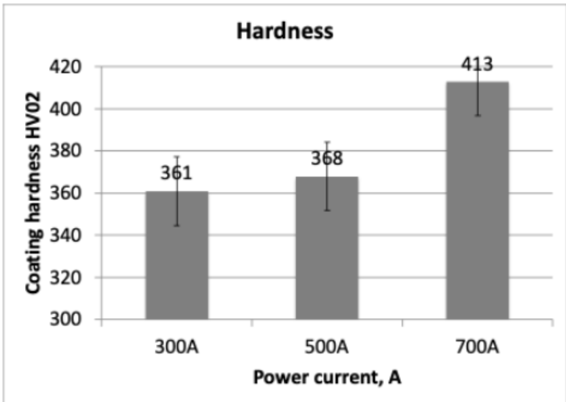

a)

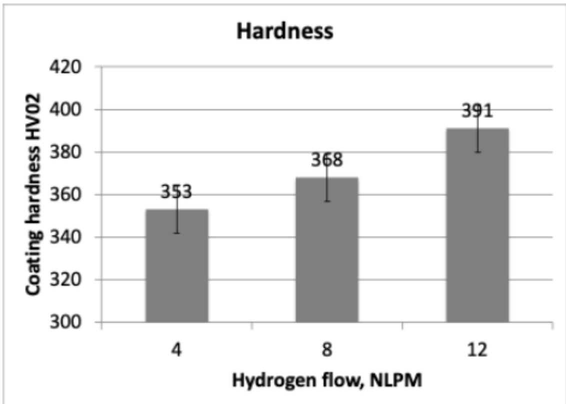

b)

Fig. 3. Influence of power current (a) and hydrogen flow (b) on hardness of plasma-sprayed NiCr-YSZ coating employing different process parameters

Erosion resistance

Erosion resistance tests conducted in accordance with ASTM G76 demonstrated that the degradation mechanism of NiCr–YSZ coatings is complex, combining features of plastic deformation of the metallic matrix with brittle fracture of the ceramic phase. The lowest mass loss (0.00703 g) was recorded for the samples produced at the increased current intensity (700 A) and hydrogen flow rate (12 NLPM), highlighting the critical role of thermal energy in the formation of erosion-resistant coatings (Fig. 4a, b). The high interlamellar cohesion and low porosity limit the "pull-out" of entire splats by impacting abrasive particles. Furthermore, the increased hydrogen flow enhances the plasticity of the NiCr matrix, enabling more effective absorption of the kinetic energy of the erodent. Alroy et al. [17] indicate that, at room temperature, the dominant erosion mechanisms in cermet coatings are micro-cutting (ploughing) and the detachment of matrix fragments along grain boundaries. The poorest erosion resistance was observed for the sample produced at the lowest current intensity (300 A), which exhibited the highest mass loss (0.01156 g), confirming the detrimental effect of porosity on the mechanical durability of the coatings. A similar trend was identified for the sample produced at a reduced hydrogen flow rate of 4 NLPM, which also resulted in significant mass loss (0.00986 g), attributed to facilitated crack propagation along structural discontinuities.

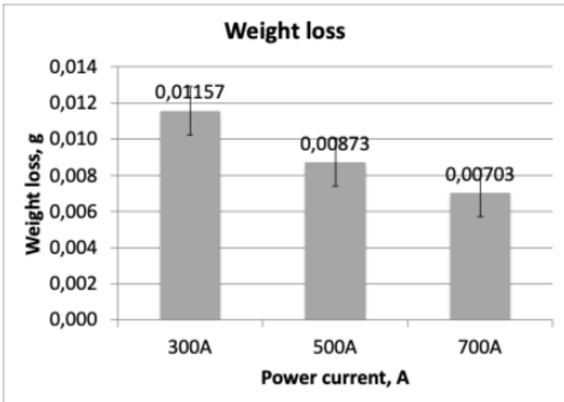

a)

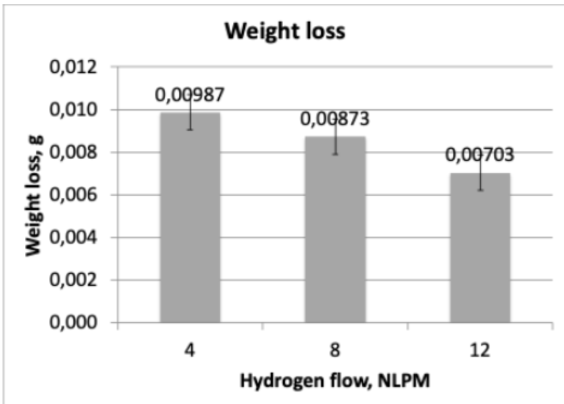

b)

Fig. 4. Influence of power (a) and hydrogen flow rate (b) on erosion resistance of plasma-sprayed NiCr-YSZ coating employing different process parameters

Sliding wear resistance

In all the cases, material loss was confined to the coating layer, with no exposure of the steel substrate. The lowest specific wear rate (8.25×10^{-5} mm³/(N·m)) was recorded for the sample sprayed at the highest current intensity (700 A), which also exhibited the highest hardness (Fig. 5a). This observation is consistent with classical Archard's law, according to which wear resistance is proportional to material hardness. Increasing the current intensity promotes the formation of a stable oxide layer at the contact interface, which may act as a glaze layer, reducing direct metal–metal contact and limiting adhesive wear. Bolelli et al. [1] demonstrated that stable oxide tribofilms significantly reduce both the coefficient of friction and the specific wear rate at elevated temperatures; a similar mechanism may occur locally under dry sliding conditions at ambient temperature owing to flash heating effects.

The highest specific wear rate was observed for the sample produced at a reduced hydrogen flow rate (4 NLPM), reaching 1.36×10^{-4} mm³/(N·m) (Fig. 5b). The pronounced decrease in wear resistance at low hydrogen flow is attributed to weak interlamellar bonding, which leads to delamination of entire coating fragments under shear forces induced by the tungsten carbide counterbody. The samples produced at the standard current intensity (500 A) and increased hydrogen flow rate (12 NLPM) exhibited comparable specific wear rates (9.73×10^{-5} and 9.80×10^{-5} mm³/(N·m), respectively), suggesting that beyond a certain plasma enthalpy threshold, further increases in hydrogen flow do not result in significant improvement in tribological performance.

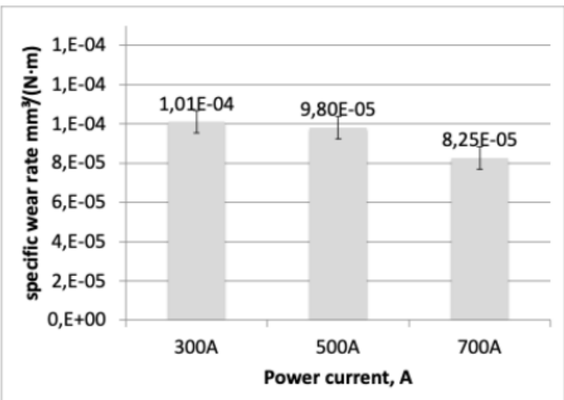

a)

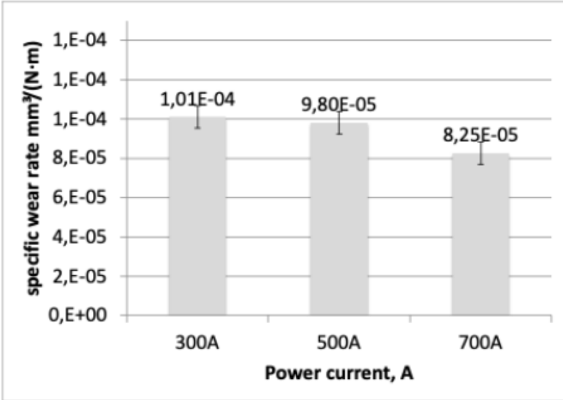

b)

Fig. 5. Effect of current (a) and hydrogen flow rate (b) on wear resistance of ball-on-disc plasma-sprayed NiCr-YSZ coating employing different process parameters

These findings are consistent with the observations of Stott et al. [18], who emphasized that surface morphology and the distribution of hard inclusions in NiCr alloys are critical factors governing the mechanical stability of the tribolayer.

CONCLUSIONS

The analysis of correlations between the processing parameters, microstructure, and functional properties of NiCr–YSZ (70/30) coatings deposited by APS indicates that the key factor governing coating quality is the plasma jet enthalpy, controlled by the torch current and hydrogen flow rate. The obtained results demonstrate that increasing the current intensity to 700 A leads to the formation of a low-porosity microstructure (0.77 vol.%), which is significantly lower than that reported for conventional plasma-sprayed NiCr coatings, for which Doleker et al. [7] reported porosity levels of approximately 1.59%. This effect is attributed to the complete melting of both the metallic matrix and Metco 6700 ceramic particles, promoting their intensive plastic deformation upon impact with the substrate and resulting in the formation of dense lamellae. An opposite trend was observed with reduced hydrogen flow, where the porosity increased to 3.17 vol.%, resulting from the lower thermal conductivity of the plasma-forming gas and the presence of numerous unmelted spheroidal particles. This observation is consistent with the findings of Savitha et al. [13], who reported that structural discontinuities in oxide-reinforced composites weaken interlamellar cohesion and accelerate coating degradation.

EDS analysis suggests phase stability of the NiCr–YSZ system, while elemental mapping revealed a heterogeneous distribution of the zirconium- and yttrium-rich ceramic phase within the Ni–Cr matrix. The mechanical properties of the coatings demonstrated a direct correlation with structural density, with the highest hardness recorded for the sample produced at 700 A, reaching 413 HV0.2. This value is significantly higher than that of the NiCr matrix alone (approximately 327 HV) [18]. In erosion resistance tests, coatings produced under the highest process energy conditions (elevated current and hydrogen flow) exhibited the lowest mass loss, which is attributed to the suppression of micro-cutting mechanisms in the metallic matrix by impacting abrasive particles.

Tribological analysis by means of the ball-on-disc method confirmed that the specific wear rate is governed by both hardness and interlamellar cohesion. The coating produced at the highest current intensity (700 A) exhibited the lowest specific wear rate (8.25×10^{-5} $mm^3/(N\cdot m)$), demonstrating the highest wear resistance. In contrast, the coating produced at the reduced hydrogen flow rate (4 NLPM) showed the highest specific wear rate (1.36×10^{-4} $mm^3/(N\cdot m)$), which is attributed to the rapid delamination and pull-out of unmelted YSZ particles as a consequence of weak interlamellar bonding under shear stresses. Overall, optimization of the plasma spraying parameters to a current intensity of 700 A and a hydrogen flow rate of 8–12 NLPM produced dense coatings with hardness exceeding 410 HV and a low specific wear rate (approximately $8–10 \times 10^{-5}$ $mm^3/(N\cdot m)$), making them well suited for operation under severe erosive–abrasive conditions.

The observed inverse relationship between the specific wear rate and coating hardness, together with the strong dependence on microstructural integrity, confirms that improved particle melting and enhanced interlamellar cohesion are the primary factors responsible for the superior tribological performance of APS-sprayed NiCr–YSZ coatings.

REFERENCES

[1] Bolelli G., Colella A., Lusvarghi L., Morelli S., Puddu P., Righetti E., et al. TiC–NiCr thermal spray coatings as an alternative to WC–CoCr and Cr_3C_2–NiCr. *Wear*. 2020;450–451:203273. https://doi.org/10.1016/j.wear.2020.203273

[2] Zhang Z., Yu Z., Yang Q., Wang Y., Yao L., Zhang T., et al. Synergistic effect of NiCr–Cr_3C_2 + Y_2O_3 on enhanced performance of Ti-based composite fabricated by laser cladding. *Mater Charact*. 2024;215:114138. https://doi.org/10.1016/j.matchar.2024.114138

[3] Góral M., Kubaszek T., Grąboń W.A., Grochalski K., Drajewicz M. The concept of WC–CrC–Ni plasma-sprayed coating with the addition of YSZ nanopowder for cylinder liner applications. *Materials*. 2023;16(3):1199. https://doi.org/10.3390/ma16031199

[4] Kubaszek T, Kościelniak B, Góral M, Hładun K, Świerk K. The influence of plasma spraying parameters on structure and properties of Stellite 31–Cr_3C_2 composite coating. *Compos Theory Pract*. 2024;54(3):181–187. https://doi.org/10.62753/ctp.2024.03.3.3

[5] Singh S., Osi A., Joshi V.V., Wade S., Berndt C.C., Schläfer T., et al. Development of fine WC–NiCr powder coatings by optimising HVOF spray parameters. *Int J Refract Met Hard Mater*. 2024;121:106667. https://doi.org/10.1016/j.ijrmhm.2024.106667

[6] Medabalimi S., Rokkala U., Gudala S., Behera N., Ramesh M.R., Dejene M. Wear and frictional behaviour of partially oxidized and plasma sprayed NiCr and NiCrBSiFe coatings. *Sci Rep*. 2025;15:99567. https://doi.org/10.1038/s41598-025-99567-8

[7] Doleker K.M., Ozgurluk Y., Parlakyigit A.S., Ozkan D., Gulmez T., Karaoglanli A.C. Oxidation behaviour of NiCr/YSZ thermal barrier coatings (TBCs). *Open Chem*. 2018;16(1):876–881. https://doi.org/10.1515/chem-2018-0096

[8] Ding F., Wei X., Cao J., Ma Y., Su H., Zhao T., et al. Thermal corrosion properties of composite ceramic coating prepared by multi-arc ion plating. *Coatings*. 2024;14(9):1150. https://doi.org/10.3390/coatings14091150

[9] Halder S., Vinay G., Anupam A., Ang A.S.M., Mahajan D.K., Singh H. Effect of prolonged immersion on corrosion and cavitation resistance of HVOF-sprayed WC–NiCr and WC–Hastelloy cermet coatings. *Surf Coat Technol*. 2024;494:131384. https://doi.org/10.1016/j.surfcoat.2024.131384

[10] Jiao X., Jia J., Zhao C., Wang J., Yang J., Cai L., et al. Tailoring micro-to-nano Cr_3C_2 ratio for enhanced hot corrosion resistance of HVOF-sprayed Cr_3C_2–NiCr cermet coatings. *Surf Coat Technol*. 2026;529:133508. https://doi.org/10.1016/j.surfcoat.2026.133508

[11] Liu F., Jia J., Yi G., Wang W., Shan Y. Mechanical and tribological properties of NiCr–Al_2O_3 composites at elevated temperatures. *Tribol Int*. 2015;84:1–8. https://doi.org/10.1016/j.triboint.2014.11.023

[12] Rakhadilov B., Buitkenov D., Sagdoldina Z., Idrisheva Z., Zhamanbayeva M., Kakimzhanov D. Preparation and characterization of NiCr/NiCr–Al_2O_3/Al_2O_3 multilayer gradient coatings by gas detonation spraying. *Coatings*. 2021;11(12):1524. https://doi.org/10.3390/coatings11121524

[13] Srinivas V., Savitha U., Reddy G.J. Processing and characterization of NiCr–YSZ compositionally graded coatings on superalloy using laser engineered net shaping (LENS). *Mater Today Proc*. 2018;5:2214–7853. (brak DOI – warto sprawdzić ręcznie)
[14] Savitha U., Srinivas V., Jagan Reddy G., Gokhale A.A., Sundararaman M. Additive laser deposition of YSZ on Ni-base superalloy for thermal barrier application. *Surf Coat Technol*. 2018;354:257–267. https://doi.org/10.1016/j.surfcoat.2018.08.089
[15] Kubaszek T., Kościelniak B., Góral M., Głód W. The influence of plasma spraying process parameters on microstructure and selected properties of novel NiCrAl–Cr_3C_2 composite coating. *Solid State Phenom*. 2026; (in press):37–44. https://doi.org/10.4028/p-8PdEdl
[16] Góral M., Kubaszek T., Kościelniak B., Stawarz D., Woźniak M. The influence of plasma spraying parameters on microstructure and hardness of aluminium–bronze–polyester–YSZ composite coatings for plain bearing applications. *Ochr Przed Koroz*. 2024;67(4):90–95. https://doi.org/10.15199/40.2024.4.1
[17] Alroy R.J., Kamaraj M., Sivakumar G. HVAF vs oxygenated HVAF spraying: Fundamental understanding to optimise Cr_3C_2–NiCr coatings for elevated temperature erosion-resistant applications. *J Mater Process Technol*. 2022;309:117735. https://doi.org/10.1016/j.jmatprotec.2022.117735
[18] Stott F.H., Lin D.S., Wood G.C., Stevenson C.W. The tribological behaviour of nickel and nickel–chromium alloys at temperatures from 20 to 800°C. *Wear*. 1976;37:1–14.

